

UC Berkeley

UC Berkeley Previously Published Works

Title

Addition to “Essentially Trap-Free CsPbBr₃ Colloidal Nanocrystals by Postsynthetic Thiocyanate Surface Treatment”

Permalink

<https://escholarship.org/uc/item/51m5w89p>

Journal

Journal of the American Chemical Society, 140(1)

ISSN

0002-7863

Authors

Koscher, Brent A
Swabeck, Joseph K
Bronstein, Noah D
[et al.](#)

Publication Date

2018-01-10

DOI

10.1021/jacs.7b13027

Peer reviewed

Essentially Trap-Free CsPbBr₃ Colloidal Nanocrystals by Postsynthetic Thiocyanate Surface Treatment

Brent A. Koscher,^{†,§,||} Joseph K. Swabeck,^{†,§,||} Noah D. Bronstein,^{†,§,||} and A. Paul Alivisatos^{*,†,‡,§,||}

[†]Department of Chemistry, University of California Berkeley, Berkeley, California 94720, United States

[‡]Department of Materials Science and Engineering, University of California Berkeley, Berkeley, California 94720, United States

[§]Materials Sciences Division, Lawrence Berkeley National Laboratory, Berkeley, California 94720, United States

^{||}Kavli Energy NanoScience Institute, University of California Berkeley and Lawrence Berkeley National Lab, Berkeley, California 94720, United States

S Supporting Information

ABSTRACT: We demonstrate postsynthetic modification of CsPbBr₃ nanocrystals by a thiocyanate salt treatment. This treatment improves the quantum yield of both freshly synthesized (PLQY \approx 90%) and aged nanocrystals (PLQY \approx 70%) to within measurement error (2–3%) of unity, while simultaneously maintaining the shape, size, and colloidal stability. Additionally, the luminescence decay kinetics transform from multiexponential decays typical of nanocrystalline semiconductors with a distribution of trap sites, to a monoexponential decay, typical of single energy level emitters. Thiocyanate only needs to access a limited number of CsPbBr₃ nanocrystal surface sites, likely representing under-coordinated lead atoms on the surface, in order to have this effect.

In recent years, lead halide perovskites have attracted considerable attention as promising optoelectronic materials for photovoltaics,^{1a,b} photodetectors,^{1c,d} and light-emitting diodes,^{1e,f} among other applications. Thin film lead halide perovskites are already in early stages of potential commercial development for photovoltaic devices. Research on their nanocrystalline counterparts lags a few years behind, but are also beginning to show promise.^{2a–c} Facile syntheses and excellent optoelectronic properties have led to the rapid emergence of cesium lead halide (CsPbX₃; X = Cl, Br, I) nanocrystals (NCs). Using solution-based procedures, CsPbX₃ NCs have been shown to present high photoluminescence quantum yields (PLQYs) of up to 90%^{3a–c} and narrow emission line widths without the need for a passivating higher band gap semiconductor shell, which is required for highly luminescent metal-chalcogenide NCs.^{4a–c}

Following this initial success, there is ongoing debate in the literature on the origin of the excellent optical performance in CsPbX₃ nanocrystals,^{5a–e} but it is generally accepted that the lead halide perovskites somewhat uniquely have a high defect tolerance. This tolerance is frequently attributed to the ionic nature of the material or the orbital composition of the energy bands that are responsible for the optical transition.^{5a–e} Although the lead halide perovskites are defect tolerant, they are not defect impervious. A number of theoretical^{6a–c} and experimental^{6a–d} studies have suggested the potential presence of non-negligible

defects in lead halide perovskites. The potential contribution of surface defects becomes increasingly important in nanocrystalline semiconductors due to the increased surface-to-volume ratio.^{4c,7a–e} The impact of these defects is most readily evident in the subunity PLQYs and extended multicomponent excited state photoluminescence (PL) decay kinetics of the CsPbX₃ nanocrystals.^{2c,3a,8a,b} These observations are consistent with the theorized shallow surface traps that would arise from a lead-rich surface.^{5a–d,6c,d} This lead-rich surface is likely due to a combination of lead-rich synthetic conditions and the lability of the oleylammonium halide surface species.^{3a,6c,8a,b} Postsynthetic processing, such as purification with antisolvents or even aging the NCs in solution, causes the PLQY to drop from 90% to 70% or lower. The PLQY deterioration is indicative of inadequate NC surface passivation, each scenario representing an opportunity for the labile surface oleylammonium halide ligands to be removed and lost.^{7c,9a}

The unusually rapid success in producing nanocrystals with 90% PLQY is encouraging; however, this begs the question: what prevents the PLQY from being unity? The presence and role of surface states in CsPbX₃ NCs has been relatively unexplored experimentally thus far. In this study, we demonstrate a surface treatment with thiocyanate that improves the PLQY of CsPbBr₃ to near unity while maintaining colloidal stability, NC shape, and crystal structure. We investigate the chemical effect of the treatment and find that no more than 10–15% of the surface ligands are replaced with thiocyanate while the stoichiometry of the NC surface changes from about 10% lead-rich to a stoichiometric 1:3 ratio of Pb to Br. We believe this treatment is an effective way of removing excess lead from the surface, consequently removing shallow traps and making the nanocrystals into near-unity green emitters.

For this investigation, colloidal CsPbBr₃ NC cubes were synthesized following the procedures developed by Protesescu et al.^{3a} with minor modifications (Supporting Information (SI) for details). The isolated as-synthesized CsPbBr₃ NCs have the desired cube-shaped morphology with typical size dispersions around \pm 10% (in edge length, determined by TEM; SI). The typical sample presents line widths comparable to single-particle line widths^{8a,b} and PLQYs between 85% and 93%, determined

Received: March 21, 2017

Published: April 27, 2017



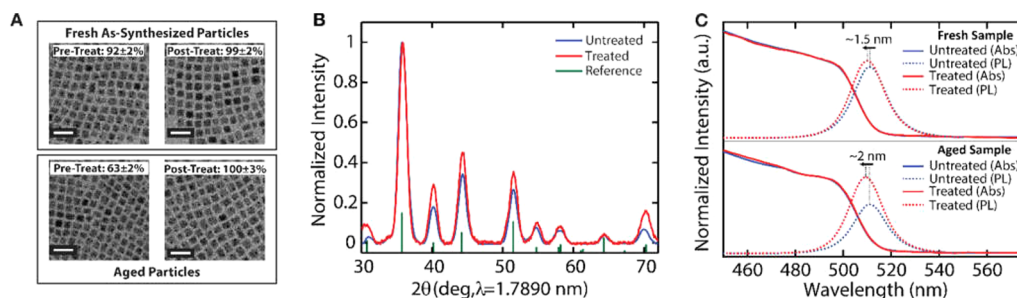


Figure 1. (A) Representative TEM images of the CsPbBr₃ NC samples before and after treatment for both fresh and aged samples, scale bar represents 25 nm. (B) X-ray diffraction patterns of the untreated (blue line) and treated (red line) aged NC sample, along with the cubic reference. (C) Absorption and photoluminescence of the fresh and aged samples both before (blue line) and after (red line) treatment.

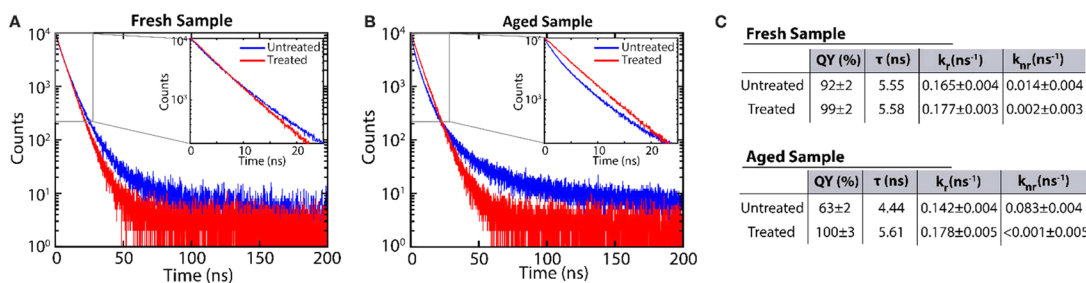


Figure 2. Time resolved photoluminescence lifetimes (Picoquant FluoTime 300) under pulsed 407.1 nm excitation (5 MHz) at room temperature for the fresh (A) and aged (B) CsPbBr₃, both before and after ammonium thiocyanate treatment. Inset figures (A and B) highlight the differences in the untreated and treated samples at early decay times. (C) Tables displaying relevant values from the PL lifetimes and PLQY, including: the PL lifetime (τ), the radiative rate (k_r), and the nonradiative rate (k_{nr}). The lifetime values of the untreated samples are amplitude weighted averages of a biexponential fit, and values for the treated sample are from a single-exponential fit.

optically using an integrating sphere (SI). Following the synthesis, samples were dispersed in anhydrous hexanes or toluene, fresh samples were used right away, and aged samples were stored for a few months first. For the thiocyanate treatment, the salt powders, either ammonium (NH₄SCN) or sodium thiocyanate (NaSCN), were added directly into the solution. The heterogeneous mixture was stirred at rt, with most optical changes occurring within the first few minutes and with little change after 20 min. Although the thiocyanate salts are added in excess, the amount of thiocyanate available in the solution at any given time is controlled by the limited solubility of the ionic salts into the nonpolar solvents. After the thiocyanate treatment, the remaining thiocyanate salt powder was removed either by using a PTFE syringe filter or by centrifugation followed by decantation. The thiocyanate salts are deliquescent and must be used dry; otherwise, the salt treatment is inconsistently effective. Powders were purchased new and maintained under dry nitrogen atmosphere. While this report focuses on NH₄SCN and NaSCN, other thiocyanate salts have not been conclusively ruled out and may also produce similar results.

Both the freshly synthesized and aged samples present uniform size distributions and regular morphologies (SI), which remains unchanged following the thiocyanate treatment, Figure 1A. The spacing between neighboring packed NCs on a TEM grid is dictated by the length and number of ligands on the surface, Figure 1A. On average, the spacing between NCs is unchanged (2.5 ± 0.1 nm before and 2.5 ± 0.2 nm after) following the thiocyanate treatment, a result that agrees with the small-angle X-ray scattering data collected on the sample (SI), indicating minimal, if any, change to the NC and ligand shell as a result of the treatment. By HR-TEM, we find that the lattice spacing is 0.58 nm before and after treatment (SI). The peak positions of the powder X-ray diffraction pattern of the NC sample remain unchanged as a

result of the treatment, Figure 1B, with peaks consistent with either a *Pm3m* or *Pnma* structure.^{9a,10} Taken together, we find that the treatment does not result in macroscopic structural changes to the NC ensemble.

While we observe essentially no macroscopic structural changes to the NCs as a result of the treatment, we find much more significant changes in the optical properties of the NCs, changes that are more pronounced in the aged than in the freshly synthesized samples. Both the aged and freshly synthesized samples exhibit symmetric and narrow PL spectra, with line widths of ~ 80 meV at fwhm, Figure 1C. However, there is a significant difference in the pretreatment PLQY of the freshly synthesized sample at $92 \pm 2\%$ and the aged sample at $63 \pm 2\%$ (SI). Following the thiocyanate treatment, the optical performance of both samples improved, boosting the PLQY to within error of unity, $99 \pm 2\%$ for the fresh sample and $100 \pm 3\%$ for the aged sample (SI). Accompanying the rise in PLQY, we find that the PL emission of the sample blue shifts by ~ 10 meV following thiocyanate treatment, Figure 1C, a small but consistently observed shift in the PL. However, we do not observe an equivalent change in the absorption spectrum following the treatment, Figure 1C, suggesting the nature of the emitting states themselves have changed slightly as a result of the thiocyanate treatment rather than being a consequence of the NCs becoming slightly smaller.

Considering the substantial improvement in the PLQY, particularly for the aged samples, the photoluminescence lifetime should show an accompanying change as a result of the treatment. Prior to thiocyanate exposure, even the freshly synthesized NCs, with a PLQY in excess of 90% following the synthesis, present PL lifetimes that are multiexponential in nature, Figure 2A. The deviation from single exponential behavior is more pronounced in the aged sample, a sample which presents a much lower PLQY,

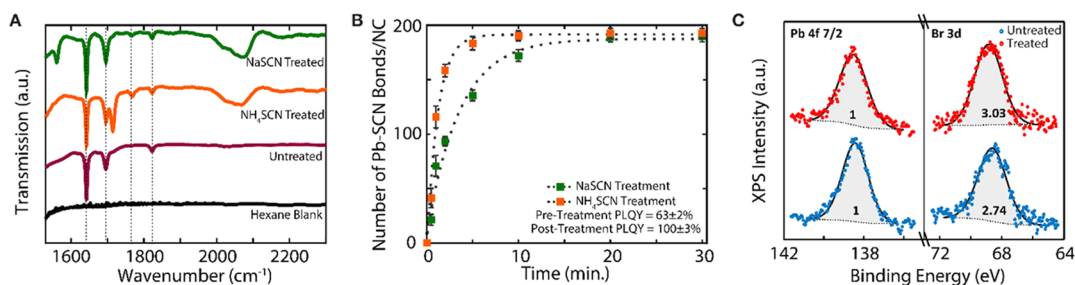


Figure 3. (A) FTIR transmission spectra for the hexanes matrix (black line), untreated (violet line), NH_4SCN treated (orange line), and NaSCN treated aged particles (green line) over the IR region of interest, between 1550 cm^{-1} to 2300 cm^{-1} . (B) Time dependent change in the number of lead-thiocyanate bonds per nanocrystal determined by focusing on the broadened peak at 2060 cm^{-1} for both the NH_4SCN and NaSCN treated particles over the course of 30 min. (C) XPS spectra of the Pb 4f 7/2 and Br 3d regions for both the untreated and treated aged sample.

Figure 2B. The observed multiexponential excited state decays are not unique to this study; indeed, it is a common feature of semiconductor NCs,^{4b,7a–e} including CsPbBr_3 NCs.^{2c,4a,6a,8a,b} When presented with a multiexponential lifetime, the interpretation is often difficult without a well-defined kinetic model of the PL decay process, and even then interpretations may be tenuous. In stark contrast, following the thiocyanate treatment we find that the PL lifetimes are highly monoexponential in character, deviating after over three decades of intensity decay ($X^2_{\text{reduced}} = 1.2$). In contrast, prior to treatment, the PL decay curves cannot be explained by a monoexponential model ($X^2_{\text{reduced}} = 9.2$). This indicates that after treatment there is a single rate-limiting step in the luminescence process, but not before, **Figure 2A,2B**. For the fresh sample, the improvement in PL decay kinetics is more subtle than the improvement in the aged system, consistent with the relatively high starting PLQY of the fresh sample ($92 \pm 2\%$), compared to the relatively lower PLQY in the aged sample ($63 \pm 2\%$). In both cases, the thiocyanate treatment is capable of minimizing the nonradiative pathways present in untreated samples, **Figure 2C**. Since the nonradiative rate is proportional to the fraction of excited states that do not luminesce, we are unable to measure it for the treated samples; their PLQY is within measurement error (2–3%) of unity. Due to the uncertainty of the PLQY measurement, we place an upper bound of 0.005 ns^{-1} on the nonradiative rate of the treated samples.

While the thiocyanate salt treatments are very effective in boosting the optical performance of the CsPbBr_3 NCs, it is of interest to examine whether sodium and ammonium thiocyanate are unique or just a member of a class of performance-enhancing species. There are two particularly notable examples in the literature, one in which the optical performance of CsPbBr_3 nanowires was improved to $\sim 50\%$ by treating with a solution of lead-oleate and oleylammonium bromide^{6e} and another where the performance of CsPbBr_3 NCs was improved using didodecyl-dimethylammonium bromide (DDAB) reaching PLQYs of $\sim 70\%$.^{6a} When we conduct the same treatments, we find comparable results (SI) to the previous literature reports^{2b,6a,b,e} but we do not observe the same level of improvement seen using a thiocyanate treatment. However, it is not unreasonable to consider that the larger sizes of these chemical species limit access to the nanocrystal surface. With this in mind, we also investigated a number of smaller molecules, particularly a number of small ammonium bromide salts. Perhaps the most promising treatment was using ammonium bromide (NH_4Br), with which we were able to observe a modest improvement in the optical performance, the PLQY going from $\sim 65\%$ to $\sim 80\%$ following treatment (SI). We investigated other potential treatments with other thiocyanate species, lead nitrate,^{2b} and other small ionic

salts (a more complete list is in the SI). From both the literature and other species we investigated, we were unable to find one that improves the optical performance to the same level as the thiocyanate, suggesting that ammonium and sodium thiocyanate are particularly advantageous, although other thiocyanate salts may result in similar improvements.

Both IR and XPS studies were performed to reveal what role thiocyanate plays on the NC surface. An easily accessible technique to identify ligand bonds on the surface of colloidal NCs, particularly the bonds of small molecules such as thiocyanate, is by using an FTIR equipped with a liquid cell sample holder to maintain colloids in the vacuum of the FTIR beam path. The bonds of greatest interest are those related to the oleate/oleic acid and thiocyanate bonds which are present in the window between 1550 and 2300 cm^{-1} . Following the thiocyanate treatment, we observe the presence of a broad peak at 2060 cm^{-1} , **Figure 3A**, consistent with the $\text{C}\equiv\text{N}$ bond of a thiocyanate bound to lead with a Pb-S bond, the position of this peak has distinctive shifts depending on the identity of the atom the thiocyanate is bound to.^{11a} When we attempted to solubilize thiocyanate salts in pure hexanes, we were not able to find IR signatures related to free thiocyanate in solution, **Figure 3A**, so any IR signatures of thiocyanate are related to thiocyanate species that are interacting with the nanoparticle in some way. The treatment with either NaSCN or NH_4SCN results in the presence of a broad thiocyanate peak at 2060 cm^{-1} , but there are additional distinctive peaks appearing depending on the counterion. Treating with NaSCN results in a peak at 1560 cm^{-1} attributed to $\text{C}=\text{O}$ stretching of sodium oleate, **Figure 3A**, while treating with NH_4SCN shows the presence of a peak at 1712 cm^{-1} attributed to the $\text{C}=\text{O}$ stretching of oleic acid. It seems that the counterion (Na , NH_4) interacts with oleate species present in the sample, while the thiocyanate interacts with lead in the nanoparticle.

A previous report showed that by treating CsPbBr_3 NCs with ammonium thiocyanate dissolved in isopropanol, all of the native ligands are exchanged with thiocyanate.^{11b} In our study, we observe a very different behavior. Rather than replacing all of the ligands, we find that there are a limited number of sites thiocyanates can access, with the $\text{C}\equiv\text{N}$ IR peak quickly growing and leveling off, representing a fraction of the total number of NC surface ligands, **Figure 3B**. In fact, if the NCs remain with excess anhydrous thiocyanate salts we find that there is no further increase in the number of lead–thiocyanate bonds per NC, even after days of exposure. This is consistent with the colloidal stability and interparticle packing of the NCs observed by TEM following the treatment. However, the situation becomes more complicated when we begin considering the surface of the nanocrystals by probing with X-ray photoelectron spectroscopy (XPS). Prior to

treatment, the aged sample has a Pb/Br ratio of 1:2.7, Figure 3C, showing that the NCs present a lead-rich surface. Following the treatment we find that the sample's Pb/Br ratio is 1:3.0, Figure 3C, the ideal ratio for CsPbBr₃ perovskites. This is very consistent with previous results, in which these lead-rich surfaces have been shown to be deleterious to optical performance^{5d,6c,9a} due to the orbital composition of the conduction band.^{5c,d,6c} However, thiocyanate treatment produces lead–thiocyanate bonds, and therefore we expect to find the appearance of a sulfur peak by XPS, but we do not (SI). The XPS results seem to suggest that the thiocyanate treatment removes excess lead atoms from the surface, removing the shallow electron traps that are harming the optical performance of the CsPbBr₃ NCs, possibly the underlying mechanism of action. However, the treatment is changing a small fraction of the lead atoms in the nanoparticle, representing at most 15% of the surface lead atoms, something that is difficult to detect, limiting the potential to understand this effect in more depth.

The findings of this communication highlight the importance and relevance of surface defects to the optical performance of the lead halide perovskites. To summarize, we have presented a thiocyanate salt treatment of CsPbBr₃ NCs that is able to very effectively decrease the nonradiative pathways of PL decay, leading to near-unity PLQYs. We find a lack of structural change accompanied by a recovery of the appropriate surface stoichiometry. We find the thiocyanate treatment is unique compared to other surface treatments in literature and similar chemical species. This treatment is able to work very effectively on both freshly synthesized and aged samples. Our data suggest that thiocyanate is able to repair a lead-rich surface, accessing a limited number of surface sites without leading to the destruction of the entire nanoparticle. While we have found success with thiocyanate treatments on CsPbBr₃ NCs, attempts to extend to other halide compositions are much less successful, with minor improvements for CsPbBr_xCl_{3-x} compositions but virtually no change from CsPbBr_xI_{3-x} compositions. We hope that future work will extend this surface-repair strategy to other lead halide perovskites, enabling unity emission across the visible spectrum.

■ ASSOCIATED CONTENT

Supporting Information

The Supporting Information is available free of charge on the ACS Publications website at DOI: 10.1021/jacs.7b02817.

Experimental section; additional figures (PDF)

■ AUTHOR INFORMATION

Corresponding Author

*E-mail: paul.alivisatos@berkeley.edu.

ORCID

Brent A. Koscher: 0000-0001-8233-0852

Joseph K. Swabeck: 0000-0003-2235-2472

A. Paul Alivisatos: 0000-0001-6895-9048

Notes

The authors declare no competing financial interest.

■ ACKNOWLEDGMENTS

This work was supported by the U.S. Department of Energy, Office of Science, Office of Basic Energy Sciences, Materials Sciences and Engineering Division, under Contract No. DE-AC02-05-CH11231 within the Physical Chemistry of Inorganic Nanostructures Program (KC3103).

■ REFERENCES

- (1) (a) Liu, M.; Johnston, M. B.; Snaith, H. J. *Nature* **2013**, *501*, 395. (b) Jeon, N. J.; Noh, J. H.; Yang, W. S.; Kim, Y. C.; Ryu, S.; Seo, J.; Seok, S. *Nature* **2015**, *517*, 476. (c) Dou, L.; Yang, Y. M.; You, J.; Hong, Z.; Chang, W.; Li, G.; Yang, Y. *Nat. Commun.* **2014**, *5*, 5404. (d) Fang, Y.; Huang, J. *Adv. Mater.* **2015**, *27*, 2804. (e) Wang, J.; Wang, N.; Jin, Y.; Si, J.; Tan, Z.; Du, H.; Cheng, L.; Dai, X.; Bai, S.; He, H.; Ye, Z.; Lai, M. L.; Friend, R. H.; Huang, W. *Adv. Mater.* **2015**, *27*, 2311. (f) Jaramillo-Quintero, O. A.; Sanchez, R. S.; Rincon, M.; Mora-Sero, I. *J. Phys. Chem. Lett.* **2015**, *6*, 1883.
- (2) (a) Zhang, X.; Sun, C.; Zhang, Y.; Wu, H.; Ji, C.; Chuai, Y.; Wang, P.; Wen, S.; Zhang, C.; Yu, W. W. *J. Phys. Chem. Lett.* **2016**, *7*, 4602. (b) Swarnkar, A.; Marshall, A. R.; Sanhira, E. M.; Chernomordik, B. D.; Moore, D. T.; Christians, J. A.; Chakrabarti, T.; Luther, J. M. *Science* **2016**, *354*, 92. (c) Li, X.; Wu, Y.; Zhang, S.; Cai, B.; Gu, Y.; Song, J.; Zeng, H. *Adv. Funct. Mater.* **2016**, *26*, 2435.
- (3) (a) Protesescu, L.; Yakunin, S.; Bodnarchuk, M. I.; Krieg, F.; Caputo, R.; Hendon, C. H.; Yang, R.; Walsh, A.; Kovalenko, M. V. *Nano Lett.* **2015**, *15*, 3692. (b) Wei, S.; Yang, Y.; Kang, X.; Wang, L.; Huang, L.; Pan, D. *Chem. Commun.* **2016**, *52*, 7265. (c) Shi, Z.; Ying, L.; Zhang, Y.; Chen, Y.; Li, X.; Wu, D.; Xu, T.; Shan, C.; Du, G. *Nano Lett.* **2017**, *17*, 313.
- (4) (a) Chen, O.; Zhao, J.; Chauhan, V. P.; Cui, J.; Wong, C.; Harris, D. K.; Wei, H.; Han, H.; Fukumura, D.; Jain, R. K.; Bawendi, M. G. *Nat. Mater.* **2013**, *12*, 445. (b) Bae, W.; Padilha, L. A.; Park, Y.; McDaniel, H.; Robel, L.; Pietryga, J. M.; Klimov, V. I. *ACS Nano* **2013**, *7*, 3411. (c) Pu, C.; Peng, X. *J. Am. Chem. Soc.* **2016**, *138*, 8134.
- (5) (a) Kang, J.; Wang, L. *J. Phys. Chem. Lett.* **2017**, *8*, 489. (b) Liu, Y.; Xiao, H.; Goddard, W. A. *Nano Lett.* **2016**, *16*, 3335. (c) ten Brinck, S.; Infante, I. *ACS Energy Lett.* **2016**, *1*, 1266. (d) Manser, J. S.; Christians, J. A.; Kamat, P. V. *Chem. Rev.* **2016**, *116*, 12956. (e) Ravi, V. K.; Markad, G. B.; Nag, A. *ACS Energy Lett.* **2016**, *3*, 7240.
- (6) (a) Pan, J.; Quan, L.; Zhao, Y.; Peng, W.; Murali, B.; Sarmah, S. P.; Yuan, M.; Sinatra, L.; Alyami, N. M.; Liu, J.; Yassitepe, E.; Yang, Z.; Voznyy, O.; Comin, R.; Hedhili, M. N.; Mohammed, O. F.; Lu, Z. H.; Kim, D.; Sargent, E. H.; Bakr, O. M. *Adv. Mater.* **2016**, *28*, 8718. (b) Pan, J.; Sarmah, S. P.; Murali, B.; Dursun, I.; Peng, W.; Parida, M. R.; Liu, J.; Sinatra, L.; Alyami, N.; Zhao, C.; Alarousu, E.; Ng, T.; Ooi, B. S.; Bakr, O. M.; Mohammed, O. R. *J. Phys. Chem. Lett.* **2015**, *6*, 5027. (c) Kim, Y.; Yassitepe, E.; Voznyy, O.; Comin, R.; Walters, G.; Gong, X.; Kanjanaboos, P.; Nogueira, A. F.; Sargent, E. H. *ACS Appl. Mater. Interfaces* **2015**, *7*, 25007. (d) Noel, N. K.; Abate, A.; Stranks, S. D.; Parrott, E. S.; Burlakov, V. M.; Goriely, A.; Snaith, H. J. *ACS Nano* **2014**, *8*, 9815. (e) Zhang, D.; Yu, Y.; Bekenstein, Y.; Wong, A. B.; Alivisatos, A. P.; Yang, P. *J. Am. Chem. Soc.* **2016**, *138*, 13155.
- (7) (a) Fischer, S.; Bronstein, N. D.; Swabeck, J. K.; Chan, E. M.; Alivisatos, A. P. *Nano Lett.* **2016**, *16*, 7241. (b) Fu, H.; Zunger, A. *Phys. Rev. B: Condens. Matter Mater. Phys.* **1997**, *56*, 1496. (c) Gao, Y.; Peng, X. *J. Am. Chem. Soc.* **2015**, *137*, 4230. (d) Zhang, H.; Yang, J.; Chen, J.; Engstrom, J. R.; Hanrath, T.; Wise, F. W. *J. Phys. Chem. Lett.* **2016**, *7*, 642. (e) Whitham, P. J.; Marchioro, A.; Knowles, K. E.; Kilburn, T. B.; Reid, P. J.; Gamelin, D. R. *J. Phys. Chem. C* **2016**, *120*, 17136.
- (8) (a) Raino, G.; Nedelcu, G.; Protesescu, L.; Bodnarchuk, M. I.; Kovalenko, M. V.; Mahrt, R. F.; Stöferle, T. *ACS Nano* **2016**, *10*, 2485. (b) Hu, F.; Zhang, H.; Sun, C.; Yin, C.; Lv, B.; Zhang, C.; Yu, W. W.; Wang, X.; Zhang, Y.; Xiao, M. *ACS Nano* **2015**, *9*, 12410.
- (9) (a) De Roo, J.; Ibáñez, M.; Geiregat, P.; Nedelcu, G.; Walravens, W.; Maes, J.; Martins, J. C.; Van Driessche, I.; Kovalenko, M. V.; Hens, Z. *ACS Nano* **2016**, *10*, 2071. (b) Pan, A.; He, B.; Fan, X.; Liu, Z.; Urban, J. J.; Alivisatos, A. P.; He, L.; Liu, Y. *ACS Nano* **2016**, *10*, 7943.
- (10) Cottingham, P.; Brutchey, R. L. *Chem. Commun.* **2016**, *52*, 5246.
- (11) (a) Fafarman, A. T.; Koh, W.; Diroll, B. T.; Kim, D. K.; Ko, D.; Oh, S. J.; Ye, X.; Doan-Nguyen, V.; Crump, M. R.; Reifsnnyder, D. C.; Murray, C. B.; Kagan, C. R. *J. Am. Chem. Soc.* **2011**, *133*, 15753. (b) Dastidar, S.; Egger, D. A.; Tan, L. Z.; Cromer, S. B.; Dillon, A. D.; Liu, S.; Kronik, L.; Rappe, A. M.; Fafarman, A. T. *Nano Lett.* **2016**, *16*, 3563.